Shear Viscosity of Two-Dimensional Yukawa Systems in the Liquid State

Bin Liu and J. Goree

Department of Physics and Astronomy, The University of Iowa, Iowa City, Iowa 52242, USA

(Received 1 February 2005; published 11 May 2005)

The shear viscosity of a two-dimensional (2D) liquid was calculated using molecular dynamics simulations with a Yukawa potential. The viscosity has a minimum at a Coulomb coupling parameter Γ of about 17, arising from the temperature dependence of the kinetic and potential contributions. Previous calculations of 2D viscosity were less extensive as well as for a different potential. The stress autocorrelation function was found to decay rapidly, contrary to earlier work. These results are useful for 2D condensed matter systems and are compared to a dusty plasma experiment.

DOI: 10.1103/PhysRevLett.94.185002 PACS numbers: 52.27.Lw, 52.27.Gr, 82.70.Dd

Two-dimensional systems in crystalline or liquid states [1] are of interest in various fields of physics. Monolayer particle suspensions can be formed in colloidal suspensions [2] and dusty plasmas [3]. Electrons on the surface of liquid helium form a 2D Wigner crystal [4]. Ions in a Penning trap can be confined as a single layer of a one-component plasma (OCP) [5]. Magnetic flux lines in 2D high-temperature superconductors form patterns of hexagonally correlated vortices [6]. At an atomic scale, gas atoms adsorb on the surface of substrates such as graphite [7]. Here we are concerned with liquids, including liquids near freezing, composed of molecules or particles that interact with a Yukawa pair potential.

The Yukawa pair potential is widely used in several fields. These include colloids, monolayer strongly coupled dusty plasmas, and some polyelectrolytes [8] in biological and chemical systems. The Yukawa potential energy for two particles of charge Q separated by a distance r is $U(r) = Q^2(4\pi\epsilon_0 r)^{-1}\exp(-r/\lambda_D)$, where λ_D is a screening length. This potential changes gradually from a long-range r^{-1} Coulomb repulsion to a hard-sphere-like repulsion as the screening parameter $\kappa = a/\lambda_D$ is increased. Here, $a = (n\pi)^{-1/2}$ is the 2D Wigner-Seitz radius [9] and n is the areal number density of particles.

The literature has only a few reports of transport coefficients computed for 2D liquids using molecular dynamics (MD) simulations. For the shear viscosity, in particular, we know of only two reports [10,11], and neither of those are for a Yukawa potential. Here we present such a simulation, yielding results for the shear viscosity and the shear stress autocorrelation function (SACF). We compare results to a recent 2D experiment [12] and to MD simulations [13–16] for the shear viscosity of 3D liquids.

Our first motivation arises from the need to model the recent dusty plasma experiment of Nosenko and Goree [12]. The experiment was performed with a horizontal monolayer of polymer microspheres suspended in a plasma, with no significant vertical motion, so that the system was 2D. The microspheres interacted with a Yukawa pair potential [17]. In an undisturbed state, particles arranged themselves in a 2D triangular lattice, which was then melted by an externally applied velocity shear due to two counterpropagating laser beams applied *in situ*. In this way, a 2D liquid was produced that had a shear flow. The experimenters measured η and found its variation with temperature.

Our second motivation is to compare η for 2D and 3D liquids, both with a Yukawa potential. Because shear viscosity has the different units of $\mathrm{kg\,m^{-1}\,s^{-1}}$ and $\mathrm{kg\,s^{-1}}$ in 3D and 2D, respectively, we divide by the volume and areal mass density, respectively, yielding the kinematic viscosity ν. This quantity has the same units of $\mathrm{m^2\,s^{-1}}$ for both 3D and 2D, thereby allowing a comparison of results for 3D and 2D.

Our simulation uses an equilibrium method to calculate η. Under equilibrium conditions, momentum transport arises from random thermal fluctuations of velocity shear in a homogeneous sample, and there is no macroscopic shear flow. Moreover, we assume that the velocity shear is small enough that η does not depend on the shear. Other types of simulations using nonequilibrium methods [13,14] would allow externally applied shear, as in the experiment.

In an equilibrium method, shear viscosity can be calculated using the Green-Kubo relation [18]. Green-Kubo formulas in general yield a macroscopic phenomenological transport coefficient, such as the viscosity or diffusion coefficient, which is written as a time integral of a microscopic time-correlation function. The Green-Kubo approach assumes that microscopic fluctuations are linear and the system has no nonequilibrium fields. Green-Kubo formulas also assume the validity of the Onsager hypothesis, i.e., that spontaneous fluctuations in microscopic quantities decay according to hydrodynamic laws, and that hydrodynamic quantities are meaningful. This requires that time scales are long compared to the collision time and that the system size is large compared to the mean free path, so that the Navier-Stokes equation and the concept of viscosity are valid.

To compute the shear viscosity, we start with time series data for the positions (x_i, y_i) and velocities $(v_{x,i}, v_{y,i})$ of N

particles, as well as the shear stress

$$P^{xy}(t) = \sum_{i=1}^{N} m v_{x,i} v_{y,i} - \sum_i \sum_{j>i} \frac{x_{ij} y_{ij} U'(r_{ij})}{r_{ij}}. \quad (1)$$

The first term of Eq. (1) is a kinetic part, which depends only on particle velocities, and the second term is a potential part, which depends on the pair potential. Here m is the particle mass and $\mathbf{r}_{ij} = (x_{ij}, y_{ij})$ is the distance between particles i and j. We can then compute the SACF

$$C_{\text{shear}}(t) = \langle P^{xy}(t) P^{xy}(0) \rangle. \quad (2)$$

Finally, we find η by integrating the SACF using the Green-Kubo relation

$$\eta = \frac{1}{A k_B T} \int_0^\infty C_{\text{shear}}(t) dt, \quad (3)$$

for a 2D liquid of area A and temperature T. Equation (3) yields the hydrodynamic parameter η based on fluctuating microscopic parameters entering into the shear stress $P^{xy}(t)$.

We use normalized units in this Letter. The length and time are normalized by a and ω_{pd}^{-1}, respectively, where $\omega_{pd} = (Q^2/2\pi\epsilon_0 m a^3)^{1/2}$ [9]. The normalized temperature is Γ^{-1}, where $\Gamma = Q^2/4\pi\epsilon_0 akT$ is the Coulomb coupling parameter, so that a high temperature corresponds to a small Γ. The 2D viscosity η is normalized by $\eta_0 = nm\omega_{pd} a^2$, and the kinematic viscosity $\nu = \eta/nm$ is normalized by $\omega_{pd} a^2$.

We performed an MD simulation to calculate η. The equations of motion for N particles were integrated using periodic boundary conditions. A thermostat was applied to achieve a constant T. We recorded particle positions and velocities, and we used Eqs. (1)–(3) to calculate η.

Our simulation model resembles the experimental system in Ref. [12]. In both of them, particles in a monolayer interact with a Yukawa potential. The values of κ and Γ were similar; all our simulations were performed for $\kappa = 0.56$ while the experiment had $\kappa = 0.53$. There are, however, significant differences. The simulation is for equilibrium conditions, while the experiment of Ref. [12], like most experiments to measure η [19], used an externally applied shear and therefore resulted in a measurement of η under nonequilibrium conditions. The simulation had periodic boundary conditions, unlike the experiment, and the equation of motion when a thermostat is used does not explicitly model the frictional damping of particle motion due to gas in the experiment.

We now review the details and tests of our simulation method. We used a velocity Verlet integrator [20] with a time step $0.02 < \Delta t < 0.05\omega_{pd}^{-1}$. We verified that Δt was small enough by performing a test, with no thermostat, where we required a fluctuation of total energy $<3\%$ over an interval of $750\omega_{pd}^{-1}$. We truncated the Yukawa potential at $r_{\text{cut}} = 22a$, with a switching function to give a smooth cutoff between $20a \le r \le 22a$. We verified that the potential energy of the entire system was almost independent of r_{cut}, for $r_{\text{cut}} > 12a$. We used $N = 1024$ particles, corresponding to a rectangle $56.99a \times 49.08a$. The size of this simulation box limits the maximum meaningful time for correlation functions to $46\omega_{pd}^{-1}$, computed as the time for a compressional sound wave to transit the box. Later we find that, except for $\Gamma > 124$, which is near freezing, the SACF decays to zero in less than $46\omega_{pd}^{-1}$, indicating that our simulation box was chosen sufficiently small. Ewald summation was not used because the simulation box was wider than λ_D by a factor of 27. The ratio of the two sides of the box were chosen to allow a perfect triangular lattice to form at high Γ.

After completing these tests, we added the Nosé-Hoover thermostat [21] to the equation of motion. We tested the thermostat with different values of the thermal relaxation time, and we chose a value of $1.0\omega_{pd}^{-1}$, which resulted in a canonical distribution within a time $4000\omega_{pd}^{-1}$. To verify that a thermal equilibrium was attained, we performed the customary test [22] of temperature fluctuations, characterized by their variance and skewness. We also verified that energy was equally partitioned among collective modes.

Our results were prepared in four steps. First, an initial configuration of random particle positions and velocities was chosen. After T reached the desired level and equilibrium was attained, we began recording data for a duration of $4 \times 10^4 \omega_{pd}^{-1}$. Second, the SACF was calculated using Eqs. (1) and (2) for the entire duration. To verify the validity of this result, we tested ten ensemble averages, each for a time series of a different duration, and we found that results for the SACF were independent of the duration, for the duration we recorded. Third, we integrated the SACF over t, yielding a value for the shear viscosity η. To verify that η does not depend on N, we calculated η using $N = 4096$ for $\Gamma = 17$ and 124, and we found that η was the same, within error bars, as for $N = 1024$. Fourth, we averaged the results for three to six different initial configurations, yielding our chief results: the SACF, as shown in Fig. 1, and η, as shown in Fig. 2(a).

The SACF decays rapidly with time for $\Gamma < 124$. This decay is almost exponential with t for large Γ, i.e., $\ln C_{\text{shear}}(t) \propto -t$. It decays even faster, $\ln C_{\text{shear}}(t) \propto -t^2$, for small Γ. These results are shown for $\Gamma = 17$ and 89 in Fig. 1. Our results are contrary to some previous results [23,24] for 2D systems, where a $C_{\text{shear}}(t) \propto t^{-1}$ dependence was found in the tail of the stress autocorrelation function. We discuss this at the end of this Letter.

We find that the shear viscosity calculated using the Green-Kubo relation is finite in 2D liquids with a Yukawa potential. This is true for a wide range of Γ, except possibly near the freezing region. This is indicated by the exponential (or faster than exponential) decay of the SACF with time in Fig. 1, so that the time integral of the SACF converges when the Green-Kubo relation is used to calcu-

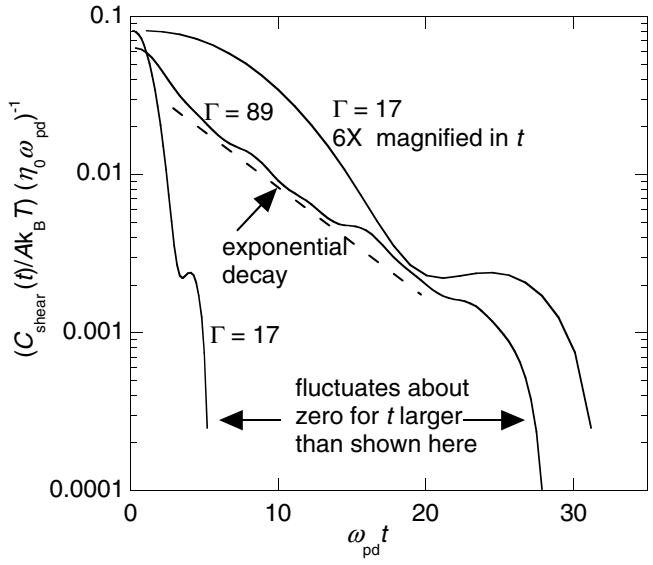

FIG. 1. Shear stress autocorrelation function $C_{\text{shear}}(t)$, computed using Eq. (2). It is significant that this function decays exponentially, or even faster, so that integrating it over time t, Eq. (3), yields a meaningful value of η.

late η. However, when the system is near freezing, i.e., $\Gamma > 124$, the decay is slower than exponential; thus, our result for η in this regime is less reliable.

Our chief result is the variation of η with Γ, Fig. 2(a). At high temperature, η decreases with Γ. In this regime, the system behaves more like a gas, as seen from the orbits [25] in Fig. 2(b). When Γ is larger than 17, on the other hand, η increases with Γ; it exhibits an exponential dependence on Γ for $\Gamma < 124$ and a much steeper increase for $\Gamma > 124$. At $\Gamma > 124$, near the freezing transition, the system has a highly ordered structure, as seen from the orbits in Fig. 2(c). The minimum viscosity, which is at $\Gamma = 17$, is $0.14\eta_0$. Using experimental parameters [12] $a = 0.6$ mm and $\omega_{pd} = 40\ \text{s}^{-1}$, our minimum corresponds to a kinematic viscosity $\nu = 2\ \text{mm}^2\,\text{s}^{-1}$ in physical units. This is about 2 times larger than the kinematic viscosity of liquid water at STP conditions. This result, as noted previously [26], is true even though η is itself an extremely small number for a dusty plasma. The reason is that the mass density is also very small, so that the kinematic viscosity, which is the ratio of these two small quantities, happens to be comparable to that of a denser substance like water.

We compare our results with the experiment of Ref. [12] in Fig. 3. As in our simulation, the experimental η varies with Γ, and it has a minimum. The minimum value $\eta = 0.13\eta_0$ in the experiment matches our result of $0.14\eta_0$.

Aside from this agreement in the magnitude of η, however, there is a difference in the value of Γ where the minimum of η occurs. The experimental result exhibits a much broader minimum, and the minimum occurs at a much higher Γ, as seen in Fig. 3. We can suggest two

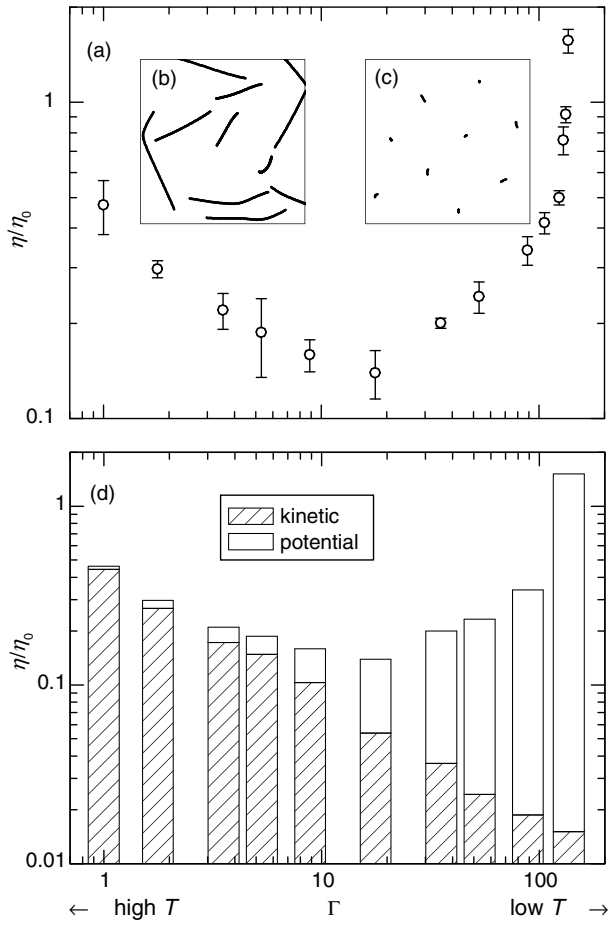

FIG. 2. (a) Simulation results show that the 2D viscosity η varies with temperature Γ^{-1}, and it has a minimum at $\Gamma = 17$. Data are shown for $\kappa = 0.56$. Error bars represent the uncertainty. (b) Particle trajectories during a time interval of $1.0\omega_{pd}^{-1}$ for $\Gamma = 1$ indicate a disordered state. (c) Particle trajectories during a time interval of $1.0\omega_{pd}^{-1}$ for $\Gamma = 124$ indicate a highly ordered structure. (d) The viscosity η is primarily the sum of two contributions: kinetic and potential.

reasons, both arising from inhomogeneity and anisotropy in the experiment that are lacking in the simulation. First, the experiment was nonequilibrium, with an applied shear that had a specific scale length and that was in a specific direction. In contrast, the simulation was in equilibrium, with the shear corresponding to thermal motions that had a wide range of length scales including very short length scales, and the direction of the shear fluctuated isotropically. Second, the experiment had a nonuniform temperature; therefore, it had nonuniform values of Γ and η, whereas the simulation was uniform. The values reported for η and Γ in experiment [12] were computed as spatial averages over a region that had a nonuniform temperature; this probably had its most significant effect on the value of Γ. Thus, it is not surprising that the Γ for the minimum in the experiment does not match that of the simulation.

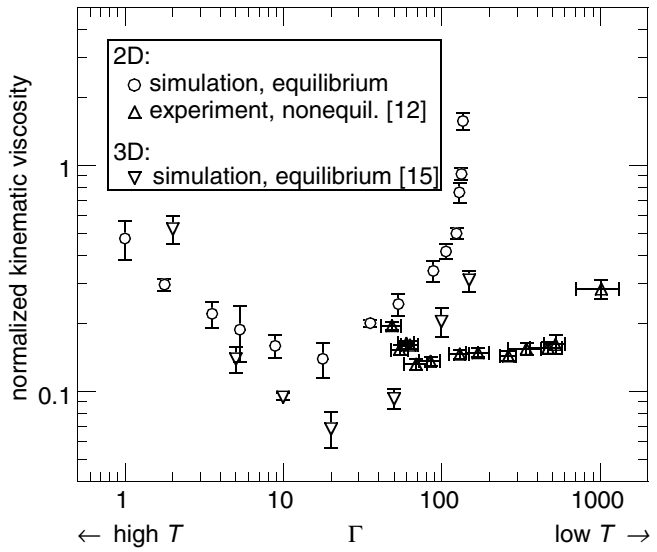

FIG. 3. Comparison of our 2D simulation with a 2D experiment and a 3D simulation. The experiment [12] used a 2D dusty plasma at $\kappa = 0.53$ with an externally applied velocity shear. The simulation of Saigo and Hamaguchi [15] used a 3D liquid with a Yukawa potential at $\kappa = 0.50$, in the absence of externally applied shear. In all three cases, η has a minimum.

To discover the effect of the dimensionality of a system, we compare the kinematic viscosity of 2D and 3D liquids. Saigo and Hamaguchi [15] performed an equilibrium simulation similar to ours, with a Yukawa potential, and their results for $\kappa = 0.5$ are plotted in Fig. 3. In both cases the viscosity has a minimum at $\Gamma \approx 20$, but the magnitudes are not the same. In 2D, the kinematic viscosity is mostly larger for the same value of Γ.

The minimum of η with temperature is a distinctive feature not found in most simple liquids. In water, for example, viscosity decreases monotonically with temperature. Systems such as strongly coupled plasmas with a long-range repulsive potential, however, tend to have a minimum. This minimum has been found in a 2D dusty plasma experiment [12], simulations of liquids with Yukawa potential in 2D (the present work) and 3D [14–16], and a simulation of a OCP [13].

The minimum arises from the temperature dependence of the kinetic and potential contributions to momentum transport. This is seen in Fig. 2(d), where the kinetic part of η decreases with Γ, while the potential part increases with Γ. (There is also a third contribution, called the cross term [18], but we found it is insignificant for our conditions.) Neither simple liquids nor dilute gases have a minimum because they are dominated by the potential and kinetic contributions, respectively.

Finally, we discuss a controversy for shear viscosity in 2D liquids. Previous theoretical and simulation efforts, with a non-Yukawa potential, yielded conflicting results for the decay of the SACF. This is important because using Green-Kubo relations to compute transport coefficients requires a decay rapid enough for the integral to converge. Previous efforts using hydrodynamic mode-coupling theory [23] and an MD simulation [24] predicted a t^{-1} dependence for the tail in the SACF; this slow decay could lead to a divergent result for the viscosity. However, other MD simulations [11] yielded a much more rapid decay, which allows the Green-Kubo integral to converge. Our result for a Yukawa potential is consistent with the latter, not the former result. This is true for $\Gamma < 124$; for $\Gamma > 124$, our data for the decay was not conclusive, so that further study with a larger simulation box and more initial conditions is needed to resolve this controversy in that range, which is very near freezing.

We thank V. Nosenko and F. Skiff for helpful discussions. This work was supported by NASA and DOE.

[1] K. J. Strandburg, Rev. Mod. Phys. **60**, 161 (1988).
[2] P. Keim, G. Maret, U. Herz, and H. H. von Grünberg, Phys. Rev. Lett. **92**, 215504 (2004).
[3] A. Melzer *et al.*, Phys. Rev. E **62**, 4162 (2000).
[4] C. C. Grimes and G. Adams, Phys. Rev. Lett. **42**, 795 (1979).
[5] T. B. Mitchell *et al.*, Phys. Plasmas **6**, 1751 (1999).
[6] P. G. Gammel *et al.*, Phys. Rev. Lett. **59**, 2592 (1987).
[7] P. W. Stephens, P. Heiney, R. J. Birgeneau, and P. M. Horn, Phys. Rev. Lett. **43**, 47 (1979).
[8] A. R. Denton, Phys. Rev. E **67**, 011804 (2003).
[9] G. J. Kalman *et al.*, Phys. Rev. Lett. **92**, 065001 (2004).
[10] W. G. Hoover and H. A. Posch, Phys. Rev. E **51**, 273 (1995).
[11] D. Gravina, G. Ciccotti, and B. L. Holian, Phys. Rev. E **52**, 6123 (1995).
[12] V. Nosenko and J. Goree, Phys. Rev. Lett. **93**, 155004 (2004).
[13] Z. Donkó and B. Nyiri, Phys. Plasmas **7**, 45 (2000).
[14] K. Y. Sanbonmatsu and M. S. Murillo, Phys. Rev. Lett. **86**, 1215 (2001).
[15] T. Saigo and S. Hamaguchi, Phys. Plasmas **9**, 1210 (2002).
[16] G. Salin and J. M. Caillol, Phys. Rev. Lett. **88**, 065002 (2002).
[17] U. Konopka, G. E. Morfill, and L. Ratke, Phys. Rev. Lett. **84**, 891 (2000).
[18] J.-P. Hansen and I. R. McDonald, *Theory of Simple Liquids* (Elsevier Academic Press, New York, 1986), 2nd ed.
[19] A. Gavrikov *et al.*, Phys. Lett. A **336**, 378 (2005).
[20] S. Toxvaerd, Mol. Phys. **72**, 159 (1991).
[21] W. G. Hoover, Phys. Rev. A **31**, 1695 (1985).
[22] B. L. Holian, A. F. Voter, and R. Ravelo, Phys. Rev. E **52**, 2338 (1995).
[23] M. H. Ernst, E. H. Hauge, and J. M. J. Van Leeuwen, Phys. Rev. Lett. **25**, 1254 (1970).
[24] G. P. Morriss and D. J. Evans, Phys. Rev. A **32**, 2425 (1985).
[25] http://dusty.physics.uiowa.edu/Movies/md.html.
[26] G. E. Morfill *et al.*, Phys. Rev. Lett. **92**, 175004 (2004).